
ELSEVIER
Volume 34, Issue 1, 2012
ISSN 0167-4730
Structural safety
An International Journal Incorporating Risk Management in the Built Environment

Structural Safety 36-37 (2012) 14–22

Contents lists available at SciVerse ScienceDirect

Structural Safety

journal homepage: www.elsevier.com/locate/strusafe

A probabilistic performance-based risk assessment approach for seismic pounding with efficient application to linear systems

E. Tubaldi [a], M. Barbato [b,*], S. Ghazizadeh [c]

[a] Dipartimento di Architettura Costruzione e Strutture, Università Politecnica delle Marche, Via Brecce Bianche, 60131 Ancona, Italy
[b] Department of Civil & Environmental Engineering, Louisiana State University and A&M College, 3531 Patrick F. Taylor Hall, Nicholson Extension, Baton Rouge, LA 70803, USA
[c] Department of Civil & Environmental Engineering, Louisiana State University and A&M College, Nicholson Extension, Baton Rouge, LA 70803, USA

ARTICLE INFO

Article history:
Received 3 April 2011
Received in revised form 16 January 2012
Accepted 16 January 2012

Keywords:
Non-stationary random processes
Separation distance
Seismic pounding
Non-classically damped systems
Performance-based earthquake engineering

ABSTRACT

Earthquake ground motion excitation can induce pounding in adjacent buildings with inadequate separation distance. The corresponding risk is particularly relevant in densely inhabited metropolitan areas, due to the usually limited separation distance between adjacent buildings.

Existing procedures to determine a minimum separation distance needed to avoid seismic pounding are based on approximations of the peak relative horizontal displacement between adjacent buildings, and are characterized by unknown safety levels. The present study proposes a probabilistic performance-based procedure for assessing the mean annual frequency of pounding between adjacent buildings. An efficient combination of analytical and simulation techniques is defined for the calculation of the pounding risk under the assumptions of linear elastic behavior for the buildings and of non-stationary Gaussian input ground motion.

The proposed methodology is illustrated by estimating the probability of pounding between linear single-degree-of-freedom systems with deterministic and uncertain properties. Furthermore, the capabilities of the proposed method are demonstrated by assessing the effectiveness of the use of viscous dampers, according to different retrofit schemes, in reducing the pounding probability of adjacent buildings modeled as linear elastic multi-degree-of-freedom systems. The results obtained based on the proposed methodology are validated against purely numerical simulation results.

1. Introduction

Earthquake ground motion excitation can induce pounding in adjacent buildings with inadequate separation distance. The corresponding risk is particularly relevant in densely inhabited metropolitan areas, due to the need of maximizing the land use and the consequent limited separation distance between adjacent buildings.

The problem of seismic pounding has been investigated by several researchers in the last two decades. A significant number of early studies focused on the definition of simplified rules, such as the Double Difference Combination rule, for determining the peak relative displacement response of adjacent buildings at the potential pounding locations [1–3]. A critical separation distance was defined and set equal to the mean peak response quantity, by neglecting the associated probability of pounding. In the same context, considerable research efforts were devoted to assessing the accuracy of the combination rules recommended in design codes (e.g., the well known absolute sum and square-root-of-the-sums-squared rules [4]) in determining the peak relative displacement response (i.e., the critical separation distance) of adjacent buildings [5].

More recent studies have adopted a probabilistic approach for the assessment of the seismic pounding risk. In Lin [6], a method was proposed to estimate the first two statistical moments of the random peak relative displacement response between linear elastic structures subjected to stationary base excitation. In Lin and Weng [7], a numerical simulation approach was suggested to evaluate the pounding probability, over a 50-year design lifetime, of adjacent buildings separated by code-specified critical separation distances. The latter study considered both the uncertainty affecting the seismic input intensity (by using a proper hazard model) and the record-to-record variability (by using artificially generated spectrum-compatible ground acceleration time histories as input loading). The buildings were modeled as multi-degree-of-freedom (MDOF) systems with inelastic behavior and deterministic properties. In Hong et al. [8], a procedure was developed to assess the fractiles of the critical separation distance between linear elastic systems with deterministic and uncertain structural properties

* Corresponding author. Tel.: +1 225 578 8719; fax: +1 225 578 4945.
E-mail addresses: etubaldi@libero.it (E. Tubaldi), mbarbato@lsu.edu (M. Barbato), sghazi1@lsu.edu (S. Ghazizadeh).

0167-4730/$ - see front matter © 2012 Elsevier Ltd. All rights reserved.
doi:10.1016/j.strusafe.2012.01.002

subjected to stationary base excitation. The previous study was later extended by Wang and Hong [9] to include non-stationary seismic input.

Despite the numerous studies available in the literature on seismic pounding, to the best of the authors' knowledge, a reliability-based methodology for the evaluation of the safety levels associated with specified critical separation distances is still needed. In addition, the gradual progress of seismic design codes from a prescriptive to a performance-based design philosophy generates a significant need for new, advanced, accurate, and computationally efficient reliability-based methodologies for the assessment and mitigation of seismic pounding risk.

This paper presents a fully probabilistic methodology for assessing the seismic pounding risk between adjacent buildings. This methodology is consistent with and can be easily incorporated into a performance-based earthquake engineering (PBEE) approach, such as the Pacific Earthquake Engineering Research center (PEER) framework [10,11]. The presented methodology considers the uncertainty affecting both the seismic input (i.e., site hazard and record-to-record variability) and the parameters used to describe the structural systems of interest (i.e., material properties, geometry, damping properties and separation distance). The seismic input is modeled as a non-stationary random process. The seismic pounding risk is computed from the solution of a first-passage reliability problem. While the performance-based approach proposed is general, the methodology presented here is specialized to linear elastic systems subjected to Gaussian loading. Under these assumptions, approximate analytical solutions and efficient simulation techniques can be used to solve the relevant first-passage reliability problem. Thus, this methodology is appropriate for structural systems that remain in their linear elastic behavior range before pounding (which is a very common condition for low values of the critical separation distances and, thus, high seismic pounding risk), although it can be extended to account for nonlinear behavior of the considered structural systems.

2. PBEE framework for seismic pounding risk assessment

The PEER PBEE framework is a general probabilistic methodology, based on the total probability theorem, for risk assessment and design of structures subjected to seismic hazard [10,11]. The PEER PBEE methodology involves four probabilistic analysis components: (1) probabilistic seismic hazard analysis (PSHA), (2) probabilistic seismic demand analysis (PSDA), (3) probabilistic seismic capacity analysis (PSCA), and (4) probabilistic seismic loss analysis (PSLA). PSHA provides the probabilistic description of an appropriate ground-motion intensity measure (*IM*), usually expressed in terms of mean annual frequency (MAF) of exceedance of a specific value *im*, $\nu_{IM}(im)$. The *IM* must be selected based on sufficiency, efficiency, and hazard computability criteria [12]. PSDA provides the statistical description of structural response parameters of interest, usually referred to as engineering demand parameters (*EDP*s), conditional to the value of the seismic intensity *IM*. PSCA consists in computing the probability of exceeding specified physical limit-states, defined by structure-specific damage measures (*DM*s), and conditional to the values of the *EDP*s. Finally, PSLA provides the probabilistic description of a decision variable (*DV*), which is a measurable attribute of a specific structural performance and can be defined in terms of cost/benefit for the users and/or the society.

The reliability-based procedure developed in this paper consists in computing the MAF of pounding between two adjacent buildings ν_p. This procedure is a specialization of the first three steps of the general PEER PBEE framework (i.e., PSLA is out of the scope of this paper) to the seismic pounding problem. It is noteworthy that the proposed approach is conceptually very different from the computation of the critical separation distance, which does not explicitly provide the probability of pounding associated with a given separation distance. The computation of the MAF of pounding can be expressed as

$$\nu_p = \int_{edp} \int_{im} G_{DM|EDP}(dm|edp) \cdot |\mathrm{d}G_{EDP|IM}(edp|im)| \cdot |\mathrm{d}\nu_{IM}(im)| \qquad (1)$$

in which $G_{DM|EDP}(dm|edp)$ = complementary cumulative distribution function of variable *DM* conditional to *EDP* = *edp*, and $G_{EDP|IM}(edp|im)$ = complementary cumulative distribution function of variable *EDP* conditional to *IM* = *im*, where upper case symbols indicate random variables and lower case symbols denote specific values assumed by the corresponding random variable.

The maximum value over time (i.e., for $t \in [0, t_{\max}]$, with t = time and $t_{\max}$ = duration of the seismic event), $U_{rel,\max}$, of the maximum relative displacement computed over the common height shared by the adjacent buildings is assumed here as *EDP*. The probabilistic distribution of $U_{rel,\max}$ reflects the record-to-record variability of the ground motions expected to occur at the site for a given intensity, as well as the effects of the uncertainty in the parameters used to describe the structural model. Finally, the pounding event is assumed as the controlling limit-state in PSCA, by using the following limit-state function, g:

$$g = \Xi - U_{rel,\max} \qquad (2)$$

in which Ξ = random variable describing the building separation distance, and the pounding event corresponds to $g \leqslant 0$. Thus, $G_{EDP|IM}(epd|im) = P[U_{rel,\max} \geqslant u | IM = im]$ and $G_{DM|EDP}(dm|edp) = P[g \leqslant 0 | U_{rel,\max} = u]$. An important intermediate result of the procedure is the convolution of PSCA and PSDA, also called fragility analysis, which yields a fragility curve. Fragility curves describe the probability $P_{p|IM}$ of pounding conditional on the seismic intensity, i.e.,

$$P_{p|IM} = \int_{edp} G_{DM|EDP}(dm|edp) \cdot \left|\mathrm{d}G_{EDP|IM}(edp|im)\right| \qquad (3)$$

The MAF of pounding, ν_p, can be used to compute the MAF of exceeding a specified value of *DV*, e.g., the MAF of repair cost due to pounding damage. The computation of the latter quantity requires the definition of a realistic loss model, based on appropriate structural response models (e.g., dynamic impact between adjacent systems) and damage models (e.g., damage produced by floor-to-floor and floor-to-column pounding). Structural response and damage models involve the definition of other *EDP*s and *DM*s, respectively, in addition to those already employed in this paper for assessing the pounding risk. Several structural response and damage models available in the literature could be employed to define an appropriate loss model [13–16].

In addition, ν_p can be directly used to determine the pounding risk, $P_p(t_L)$, for a given structure over its design life (t_L = design lifetime, e.g., 50 years). Assuming that the occurrence of a pounding event can be described by a Poisson process and that the buildings are immediately restored to their original condition after pounding occurs, $P_p(t_L)$ can be easily computed as

$$P_p(t_L) = 1 - e^{-\nu_p \cdot t_L} \qquad (4)$$

3. Seismic pounding risk assessment methodology

Fragility analysis is the most computationally challenging component of the probabilistic PBEE framework. A simple and general approach for fragility analysis in seismic pounding assessment is provided by Monte Carlo simulation [5,7]. For any given value of *IM*, Monte Carlo simulation-based fragility analysis requires (1) the definition of a set of ground motions that are selected from an appropriate database of real records or generated from an appropriate random process, (2) the sampling of the parameters that define the structural systems and their separation distances, (3) the numerical simulation of the structural response for each ground motion time history and each set of structural parameters and separation distances, and (4) the evaluation of $P_{p|IM}$ as the ratio between the number of failures and the number of samples. However, the computational cost associated with Monte Carlo simulation can be very high and even prohibitive when small failure probabilities need to be estimated by numerically simulating the time history response of complex and/or large-scale MDOF systems.

In this paper, an efficient combination of analytical and simulation techniques is proposed for the calculation of $P_{p|IM}$ under the assumptions of linear elastic behavior for the buildings and of Gaussian input ground motion. The methodology is described first for linear elastic systems with deterministic structural properties and separation distance, and then generalized to stochastic linear systems.

It is noteworthy that, for low values of the building separation distance ξ, the buildings are expected to behave elastically before pounding occurs. The assumption of linear behavior of the buildings before pounding becomes less realistic for larger values of ξ and may result in an underestimation of the pounding risk, particularly for buildings with fundamental periods shorter than approximately 1.0 s. This underestimation is due to the fact that, in general, inelastic displacements are expected to be larger than those evaluated with elastic models. If the buildings are expected to yield before pounding, their nonlinear structural behavior must be accounted for by extending the methodology described in the remainder of this paper, e.g., by using statistical linearization techniques [17] or subset simulation [18]. This extension is out of the scope of this paper.

3.1. Linear systems with deterministic structural properties

The computation of the conditional failure probability $P_{p|IM}$ can be expressed in the form of a single-barrier first-passage reliability problem as [5,9]

$$P_{p|IM} = P\left\{ \max_{0 \leqslant t \leqslant t_{\max}} [U_{rel}(t)] \geqslant \xi \middle| IM = im \right\} \tag{5}$$

in which $U_{rel}(t) = \max_{0 \leqslant y \leqslant h} [U_{A,y}(t) - U_{B,y}(t)] \approx U_{A,h}(t) - U_{B,h}(t)$; $U_{A,y}(t)$ and $U_{B,y}(t)$ = displacement response of the adjacent buildings A and B at elevation y; h = roof elevation of the shorter building, usually assumed as the most likely pounding location [1–3,6,7]; and ξ = deterministic value of the building separation distance (Fig. 1).

Under the hypotheses of deterministic linear elastic systems subjected to Gaussian loading processes and of deterministic threshold, several analytical approximations of $P_{p|IM}$ exist in the literature [19–22]. These analytical approximations require computing the following statistics of the relative displacement process $U_{rel}(t)$ for a given $IM = im$: $\sigma^2_{U_{rel}}(t)$ = variance of $U_{rel}(t)$, $\sigma^2_{\dot{U}_{rel}}(t)$ = variance of the relative velocity process $\dot{U}_{rel}(t)$, $\rho_{U_{rel}\dot{U}_{rel}}(t)$ = correlation coefficient between $U_{rel}(t)$ and $\dot{U}_{rel}(t)$, and $q_{U_{rel}}(t)$ = bandwidth parameter of $U_{rel}(t)$. These statistics can be obtained from the zero-th, first, and second order spectral characteristics of process $U_{rel}(t)$ [23–25]. Following the methodology described in Barbato and Conte [24], a state-space formulation of the equations of motion for the two buildings is employed to compute exactly and in closed-form the required spectral characteristics. The approach followed here is based on random vibration theory (similar to existing stochastic techniques for the derivation of analytical fragility curves [28,29]) and effortlessly accounts for the record-to-record variability of the seismic input.

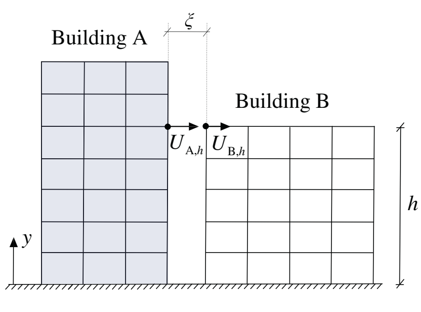

Fig. 1. Geometric description of the pounding problem between adjacent buildings.

The seismic input is modeled as a time-modulated Gaussian colored noise process. This analytical representation of the seismic input requires the definition of a power spectral density and of a time-modulating function [25]. The parameters needed to define analytically the power spectral density and the time-modulating function can be calibrated to represent the characteristics of the seismic input expected at the site [26] or to match a code-specified response spectrum [27]. For the specific input ground motion process considered in this paper, the spectral characteristics of the displacement processes (and of any response process obtained as a linear combination of the displacement processes) are available in exact closed-form for single-degree-of-freedom (SDOF) systems and both classically and non-classically damped MDOF systems [25]. It is noteworthy that the general framework presented in this paper can be used in conjunction with any representation of the earthquake ground motion, e.g., with a set of properly selected and scaled recorded ground motions [30], as commonly done in PEER PBEE [10,11]. However, the efficient methodology introduced here for the pounding probability assessment of linear elastic systems requires an analytical representation of the earthquake ground motion through an appropriate random process. In addition, the IM must be selected so that it can be readily related to the stochastic description of the seismic input.

The equations of motion for the linear system constituted by two non-connected adjacent buildings can be expressed as follows:

$$\mathbf{m} \cdot \ddot{\mathbf{U}}(t) + \mathbf{c} \cdot \dot{\mathbf{U}}(t) + \mathbf{k} \cdot \mathbf{U}(t) = \mathbf{p} \cdot F(t) \tag{6}$$

in which $\mathbf{m} = \begin{pmatrix} \mathbf{m}_A & \mathbf{0} \\ \mathbf{0} & \mathbf{m}_B \end{pmatrix}$, $\mathbf{c} = \begin{pmatrix} \mathbf{c}_A & \mathbf{0} \\ \mathbf{0} & \mathbf{c}_B \end{pmatrix}$, $\mathbf{k} = \begin{pmatrix} \mathbf{k}_A & \mathbf{0} \\ \mathbf{0} & \mathbf{k}_B \end{pmatrix}$, $\mathbf{U} = \begin{pmatrix} \mathbf{U}_A \\ \mathbf{U}_B \end{pmatrix}$; $\mathbf{m}_i$, $\mathbf{k}_i$, $\mathbf{c}_i$ and $\mathbf{U}_i$ = mass matrix, damping matrix, stiffness matrix, and vector of nodal displacements of building i, respectively (i = A, B); $\mathbf{p}$ = load distribution vector; $F(t)$ = scalar function describing the time-history of the external loading (input random process); and a superposed dot denotes differentiation with respect to time. It is noteworthy that connections between the two buildings (e.g., damping devices interposed between the buildings to mitigate seismic pounding risk) can be easily modeled by introducing the appropriate terms in matrix $\mathbf{c}$. The response process $U_{rel}(t)$ can be related to the displacement response vector $\mathbf{U}(t)$ by means of a linear operator $\mathbf{b}$, i.e., $U_{rel}(t) = \mathbf{b} \cdot \mathbf{U}(t)$.

For the sake of clarity, the same earthquake input $F(t) = -\ddot{x}_g(t)$ is applied as base excitation to both building A and B, i.e., the effects of asynchronous ground motion are ignored. This assumption, in general, can lead to an underestimation of the relative displacement of adjacent structures and of the corresponding pounding probability. However, for the problem considered in this paper, this assumption is expected to have negligible effects, since the pounding risk is relevant only when the adjacent buildings are very close. It is noteworthy that the effects of asynchronous ground motion on the assessment of the pounding probability can be easily included in the framework proposed in this paper by using an appropriate coherency function, e.g., following the approach presented in Hao and Zhang [31].

The probability of pounding conditional on $IM = im$ corresponds to the solution of a first-passage reliability problem and is given by [32]

$$P_{p|IM} = 1 - P[U_{rel}(t=0) < \xi | IM = im] \cdot \exp\left\{-\int_0^{t_{\max}} h_{U_{rel}|im}(\xi,\tau)\cdot \mathrm{d}\tau\right\} \quad (7)$$

in which $P[U_{rel}(t = 0) < \xi|IM = im]$ = probability that the random process $U_{rel}(t)$ is below the threshold ξ at time $t = 0$ s, and $h_{u_{rel}|im}(\xi,t)$ = time-variant hazard function conditional on $IM = im$. For systems with at rest initial conditions, $P[U_{rel}(t = 0) < \xi|IM = im] = 1$.

To date, no exact closed-form expressions exist for the time-variant hazard function $h_{U_{rel}|im}(\xi,t)$. However, several approximate solutions are available in the literature, e.g., Poisson's (P), $h^{(\mathrm{P})}_{U_{rel}|im}(\xi,t) = \nu_{U_{rel}|im}(\xi,t)$, classical Vanmarcke's (cVM), $h^{(\mathrm{cVM})}_{U_{rel}|im}(\xi,t)$, and modified Vanmarcke's (mVM), $h^{(\mathrm{mVM})}_{U_{rel}|im}(\xi,t)$, approximations [22,33,34]. These analytical approximations can be readily computed based on the closed-form expressions of the spectral characteristics of process $U_{rel}(t)$, as shown in Barbato and Vasta [25]. In addition, for linear elastic systems subjected to Gaussian loading, $P_{p|IM}$ can be efficiently and accurately estimated by using the Importance Sampling using Elementary Events (ISEE) method [35].

3.2. Linear systems with uncertain structural properties and separation distance

In addition to the uncertainty in the seismic input, significant uncertainty can be found in geometrical, mechanical, and material properties characterizing the structural systems and their models. Hereinafter, the uncertainty in geometrical, mechanical, and material properties of the structural models, as well as in their separation distance, Ξ, is referred to as model parameter uncertainty. Model parameter uncertainty can significantly modify the structural performance and, thus, must be considered in the assessment of seismic pounding risk.

In order to include the effects of model parameter uncertainty, the total probability theorem is employed to compute the conditional probability of pounding as follows:

$$P_{p|IM} = \int_{\mathbf{X}} P_{p|IM,\mathbf{X}}(\mathbf{x})\cdot f(\mathbf{x})\cdot \mathrm{d}\mathbf{x} = E_{\mathbf{X}}[P_{p|IM,\mathbf{X}}] \quad (8)$$

in which $\mathbf{X}$ = vector of uncertain model parameters (including the uncertain separation distance Ξ) with joint probability density function $f_{\mathbf{X}}(\mathbf{x})$, and $P_{p|IM,\mathbf{X}}(\mathbf{x})$ = probability of pounding conditional on $\mathbf{X}$ and IM.

Monte Carlo simulation, or any variance reduction technique such as stratified sampling, can be employed to evaluate $P_{p|IM}$ in Eq. (8). For example, Latin hypercube sampling can be employed for its computational efficiency [36]. The samples of $\mathbf{X}$ generated by employing Latin hypercube sampling can be used to define a set of deterministic linear elastic models with deterministic separation distance, for which the conditional probability of pounding can be computed as in Eq. (7).

4. Application examples

In this section, the proposed methodology is applied to: (1) compute the pounding risk for SDOF systems with deterministic model parameters, (2) compute the pounding risk for SDOF systems with uncertain model parameters, and (3) evaluate the effectiveness of different retrofit solutions using viscous dampers in reducing the pounding risk for deterministic MDOF models of multistory buildings.

In all the application examples considered here, the input ground acceleration is modeled by a time-modulated Gaussian process. The time-modulating function, $I(t)$, is represented by the Shinozuka–Sato's function [37], i.e.,

$$I(t) = c\cdot(e^{-b_1\cdot t} - e^{-b_2\cdot t})\cdot H(t) \quad (9)$$

in which $b_1 = 0.045\pi$ s^{-1}, $b_2 = 0.050\pi$ s^{-1}, $c = 25.812$, and $H(t)$ = unit step function. A duration $t_{\max} = 30$ s is considered for the seismic excitation.

The power spectral density of the embedded stationary process is described by the widely-used Kanai-Tajimi model, as modified by Clough and Penzien [38], i.e.,

$$S_{CP}(\omega) = S_0\cdot\frac{\omega_g^4 + 4\cdot\xi_g^2\cdot\omega^2\cdot\omega_g^2}{[\omega_g^2-\omega^2]^2 + 4\cdot\xi_g^2\cdot\omega^2\cdot\omega_g^2}\cdot\frac{\omega^4}{[\omega_f^2-\omega^2]^2 + 4\cdot\xi_f^2\cdot\omega^2\cdot\omega_f^2} \quad (10)$$

in which S_0 = amplitude of the bedrock excitation spectrum, modeled as a white noise process; ω_g and ξ_g = fundamental circular frequency and damping factor of the soil, respectively; and ω_f and ξ_f = parameters describing the Clough–Penzien filter. The values of the parameters employed for all the applications are ω_g = 12.5 rad/s, $\xi_g = 0.6$, ω_f = 2 rad/s, and $\xi_f = 0.7$. The power spectral density function in Eq. (10) is shown in Fig. 2a for $S_0 = 1$ m^2/s^3.

The choice of an appropriate IM for the seismic pounding problem is a crucial step for the proposed performance-based methodology. The spectral acceleration $S_a(T_1)$ at the fundamental period of vibration is often used as the IM for the evaluation of the seismic response of buildings. In fact, for single buildings with deterministic properties (i.e., deterministic natural period, T_1), $S_a(T_1)$ has been found to be a sufficient and highly efficient IM [39]. However, in the problem considered in this paper, the fundamental periods of vibration of both buildings contribute significantly to the relative displacement and, thus, to the probability of pounding. Therefore, $S_a(T_1)$ (in which T_1 denotes the fundamental period of one of the two buildings) is not a sufficient and efficient IM. The efficiency of $S_a(T_1)$ is further reduced when considering modeling uncertainties (i.e., when the natural periods of the structures are uncertain [40]). It is noteworthy that the proposed formulation has no limitations in terms of the choice of the IM. In this context, a vector-valued IM based on a combination of the spectral accelerations corresponding to the natural periods of the two adjacent buildings appears to be a potentially highly efficient IM [12,41,42]. However, an in-depth analysis of the sufficiency and efficiency of different IMs is beyond the scope of this paper. Therefore, the peak ground acceleration (PGA) is assumed here as the IM for the sake of simplicity. In order to derive the fragility curves in terms of the selected IM, the relationship between the parameter S_0 of the Kanai-Tajimi spectrum and the PGA at the site is assessed empirically. A set of 500 synthetic stationary ground motion records are generated using the spectral representation method [43] based on the power spectral density function given in Eq. (10) with $S_0 = 1$ m^2/s^3. Each ground motion realization is then modulated in time using the function defined in Eq. (9). The peak ground acceleration corresponding to $S_0 = 1$ m^2/s^3, $PGA_{S_0=1}$, is estimated as the mean of the PGAs of the sampled ground motion time histories. The values of S_0 corresponding to different values of PGA are obtained as follows:

$$S_0 = \left(\frac{PGA}{PGA_{S_0=1}}\right)^2 \quad (11)$$

In this study, the site hazard curve is expressed in the approximate form used in Cornell et al. [44], i.e.,

$$\nu_{IM}(im) = P[IM \geqslant im|1yr] = k_0\cdot im^{-k_1} \quad (12)$$

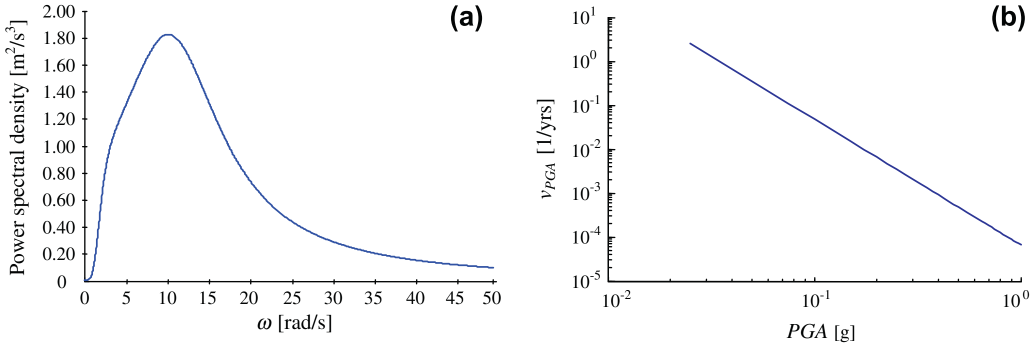

Fig. 2. Input ground motion: (a) power spectral density function of the embedded stationary process, and (b) site hazard curve.

in which k_0 and k_1 = parameters obtained by fitting a straight line through two known points of the site hazard curve plotted in logarithmic scale. For the applications presented in this paper, the site hazard curve is taken from Eurocode 8-Part 2 [45], assuming that PGA = 0.3 g corresponds to a return period of 475 years for the site of interest. Using k_1 = 2.857 [46], the site hazard curve becomes (see Fig. 2b)

$$\nu_{PGA}(pga) = 6.734 \times 10^{-5} \cdot pga^{-2.857} \quad (13)$$

4.1. Pounding risk for linear SDOF systems with deterministic model parameters

The first application example consists in the assessment of the pounding risk between two adjacent buildings modeled as deterministic linear elastic SDOF systems with periods T_A and T_B and damping ratios $\zeta_A = \zeta_B$ = 5%. In order to realistically represent the behavior of actual building structures, the properties of the two SDOF systems need to be chosen appropriately. A possible approach to achieve this objective is the one proposed by Penzien [3], in which a linear displacement assumption is employed to relate the displacement of a MDOF system at the pounding location to the displacement of a corresponding generalized SDOF system. It is noted that the results presented here are independent of the technique that is employed to relate the SDOF and MDOF system responses. The conditional probability of pounding $P_{p|IM}$ is calculated using the approximate analytical hazard functions $h^{(\mathrm{P})}_{U_{rel}|im}(\xi,t)$, $h^{(\mathrm{cVM})}_{U_{rel}|im}(\xi,t)$, and $h^{(\mathrm{mVM})}_{U_{rel}|im}(\xi,t)$, for a deterministic distance between the buildings ξ = 0.1 m and for two different combinations of natural periods of the two systems, i.e., (1) T_A = 1.0 s and T_B = 0.5 s, referred to as well separated natural periods (Fig. 3a), and (2) T_A = 1.0 s and T_B = 0.9 s, referred to as close natural periods (Fig. 3b). The obtained conditional probabilities are presented in Fig. 3 as fragility curves and compared with the corresponding results obtained using the ISEE method [35], which are assumed as reference solution.

In the case of well separated natural periods for the structures (Fig. 3a), the fragility curves estimated using the P, cVM, and mVM approximations are very similar and close to the fragility curves obtained using the ISEE method. In the case of close natural periods (Fig. 3b), the fragility curves estimated with the approximate analytical methods show significant differences, and only the cVM approximation provides results that are close to the fragility curves estimated using the ISEE method. The observed result can be explained by recognizing that the relative displacement process $U_{rel}(t)$ can be interpreted as a response process of a two-degree-of-freedom system. This multi-modal characteristic of $U_{rel}(t)$ can significantly affect the accuracy of the different approximations of the time-variant hazard function $h_{U_{rel}|im}(\xi,t)$ [47]. In the case of well separated natural periods, the contribution to $U_{rel}(t)$ of the vibration mode with higher period is significantly larger than the contribution of the vibration mode with lower period. By contrast, in the case of close natural periods, both vibration modes provide a significant contribution to the response process.

Fig. 4 shows the MAF of pounding, ν_p, as a function of the building separation distance ξ (in semi-logarithmic scale) for the cases of well separated natural periods (Fig. 4a) and of close natural periods (Fig. 4b), respectively. The estimates of the MAF of pounding obtained using the analytical approximations (P, cVM, and mVM) of the hazard function are compared to the corresponding estimate obtained using the ISEE method. Fig. 5 plots (in semi-logarithmic scale) the pounding risk for a design lifetime of 50 years, evaluated according to Eq. (4), for the same two cases of well separated and

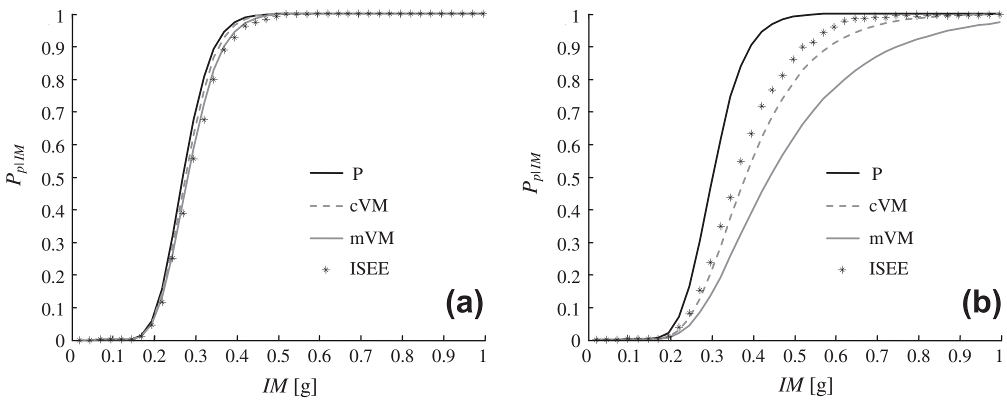

Fig. 3. Fragility curves for ξ = 0.1 m: (a) T_A = 1.0 s and T_B = 0.5 s, and (b) T_A = 1.0 s and T_B = 0.9 s.

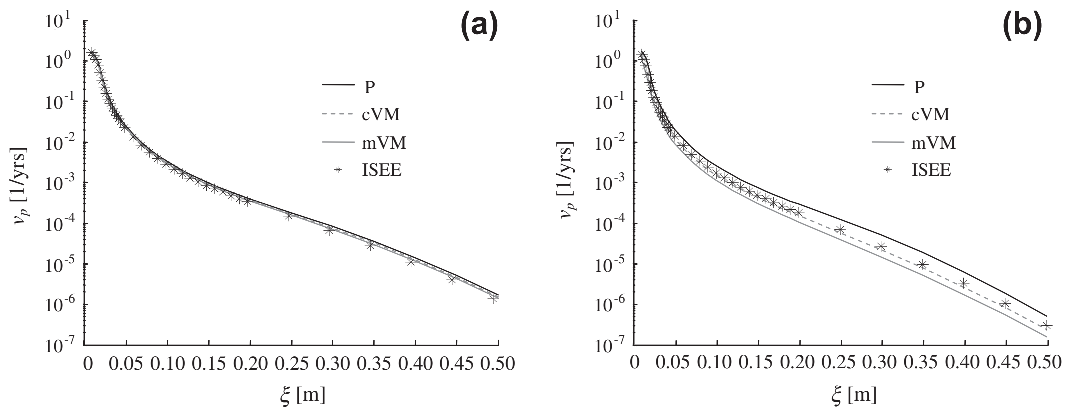

Fig. 4. MAF of pounding for varying separation distance: (a) T_A = 1.0 s and T_B = 0.5 s, and (b) T_A = 1.0 s and T_B = 0.9 s.

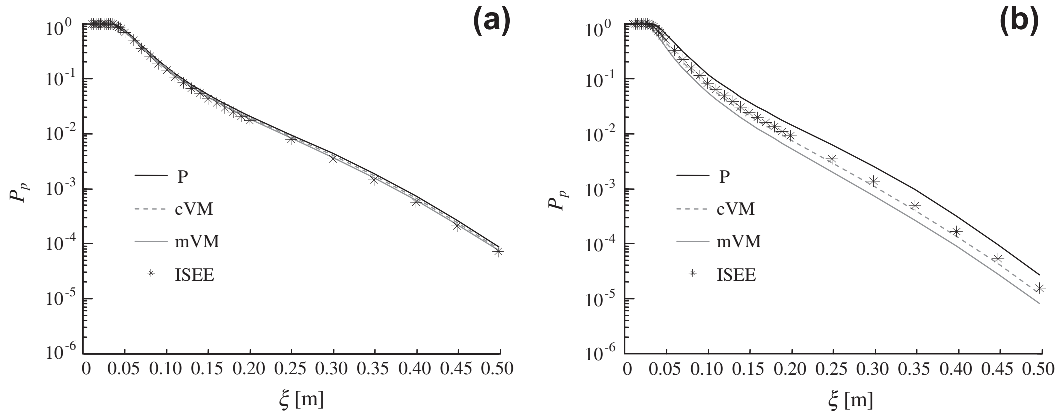

Fig. 5. 50-year pounding risk for varying separation distance: (a) T_A = 1.0 s and T_B = 0.5 s, and (b) T_A = 1.0 s and T_B = 0.9 s.

close natural periods. Considerations similar to the ones made for the fragility curves can be made also for the MAF of pounding and the 50-year pounding risk, i.e., the analytical approximations provide very accurate results for the case of well separated natural periods and less accurate results for the case of close natural periods, with the exception of the cVM approximation, which is accurate in both cases.

It is observed that the P approximation of the time-variant hazard function always yields conservative results; while the mVM approximation underestimates the risk computed using the ISEE method for the case of close natural periods. Similar results have been documented for the first-passage reliability problem of SDOF and MDOF systems subjected to time-modulated white and colored noise excitations [33,34].

4.2. Pounding risk for SDOF systems with uncertain model parameters

The effects of model parameter uncertainty on the pounding probability are investigated in this second application example. In order to include uncertainty in the stiffness, inertia, and dissipative properties of the two SDOF systems [8,9], their natural periods are modeled as independent lognormal random variables with mean values equal to 1.0 s and 0.5 s, respectively, and coefficients of variation equal to 0.3, while the damping ratios are modeled as independent lognormal random variables with mean values equal to 0.05 and coefficients of variation equal to 0.5. The statistical description of the random separation distance Ξ is obtained based on the interstory out-of-plumbness of the columns at each floor of the two buildings [48]. The influence of the columns' out-of-plumbness on the stiffness of the structural systems is neglected.

In this application example, building A is a 10-story building and building B is a 5-story building, both with a constant interstory height equal to 3.00 m. The interstory out-of-plumbness Θ at each floor of each building are modeled as independent normal random variables with mean $\mu_\Theta = 0.0$ rad and standard deviation $\sigma_\Theta = 0.0015$ rad [48]. Thus, the separation distance Ξ at the roof level of building B is a normal random variable with mean value μ_Ξ equal to the nominal value of the buildings' distance and standard deviation $\sigma_\Xi = 0.0142$ m. In order to account for the variability of these model parameters, a total of 50 samples of the vector $\mathbf{X}$ is generated using the Latin hypercube sampling technique [36].

Fig. 6a plots the pounding probability conditional to $IM = im$ (in short, fragility curve) corresponding to (1) deterministic SDOF systems with deterministic separation distance, (2) SDOF systems with deterministic separation distance and uncertain periods and damping ratios, and (3) SDOF systems with uncertain natural periods, damping ratios, and separation distance. For the sake of clarity, only the fragility curves obtained using the mVM approximation of the time-variant hazard function are shown. It is observed that model parameter uncertainty increases the dispersion of the response of the two SDOF systems, and thus the corresponding fragility curves, while the shift of the IM corresponding to 50% probability of pounding is negligible. The uncertainty affecting the separation distance Ξ has a practically negligible effect on the pounding probability for the considered values of the separation distance.

Fig. 6b shows the 50-year probability of pounding as a function of the separation distance, for the same three cases considered in

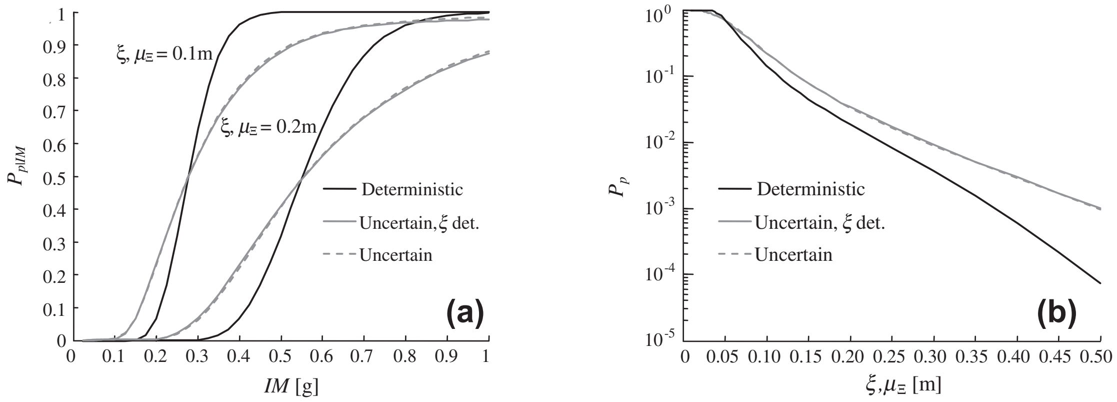

Fig. 6. Effects of model parameter uncertainty on pounding risk for SDOF systems: (a) fragility curves for threshold levels of 0.1 m and 0.2 m, and (b) 50-year pounding risk for different threshold levels.

Fig. 6a. It is observed that model parameter uncertainty increases the pounding risk for separation distances higher than 0.06 m. This phenomenon can be explained considering that, when model parameter uncertainty is considered and $\mu_\Xi > 0.06$ m, the fragility curve is higher for lower *IM* values (with higher MAF) and lower for higher *IM* values (with lower MAF) than when model parameter uncertainty is neglected (see Fig. 6a). The observed underestimation of the pounding risk due to neglecting model parameter uncertainty is non-negligible and can be as high as 35% for a large range of separation distances. This result suggests that the effects of model parameter uncertainty be included in the assessment of the pounding risk, particularly when a high degree of uncertainty affects the model parameters.

4.3. MDOF models of multistory buildings retrofitted by using viscous dampers

As a third application, the proposed methodology is employed to assess the risk of pounding between two adjacent multistory buildings modeled as linear MDOF systems, before and after retrofit with viscous dampers. Different retrofit solutions are considered and their effectiveness in reducing the seismic pounding risk is compared. The considered buildings are steel moment-resisting frames with shear-type behavior. The properties of the buildings are taken from Lin [49]. Building A is an 8-story building with story stiffness k_A = 628,801 kN/m (equal for every story) and floor mass m_A = 454.545 tons (equal for each floor), building B is a four-story building with story stiffness k_B = 470,840 kN/m and floor mass m_B = 454.545 tons. A Rayleigh-type damping matrix $\mathbf{c_R}$ is used (see Eq. (6)) to model the inherent buildings' damping and is built by considering a damping ratio ζ_R = 2% for the first two vibration modes of each system. Model parameter uncertainty is not considered in this application. The fundamental vibration periods of building A and B are T_A = 0.915 s and T_B = 0.562 s, respectively.

The following six different retrofit solutions, based on the use of braces with purely viscous behavior [50], are considered: (1) braces located at each story of both buildings (retrofit scheme 1), (2) braces located at the lower four stories of both buildings (retrofit scheme 2), (3) braces located at all stories of the short building only (retrofit scheme 3), (4) braces located at all stories of the tall building only (retrofit scheme 4), (5) braces located at the lower four stories of the tall building only (retrofit scheme 5), and (6) braces located at the first story of the tall building only. The two buildings before retrofit are shown in Fig. 7a, while the six retrofit schemes are shown in Fig. 7b. The viscous braces provide an additional source of damping, modeled by means of a damping matrix $\mathbf{c_V}$. The total damping matrix for the system constituted by the two buildings is $\mathbf{c} = \mathbf{c_R} + \mathbf{c_V}$. The damping coefficient corresponding to the dampers at each floor of buildings A and B is c_d = 10,000 kN s/m. The systems corresponding to retrofit schemes 2, 5, and 6 are non-classically damped and their analysis requires the use of the complex modal analysis technique [25].

Fig. 8a shows three different analytical estimates (P, cVM, and mVM approximations) of the 50-year probability of pounding between the two buildings before retrofit. The 50-year probability of pounding is plotted for different values of the separation distance. Fig. 8a also reports the 50-year probability of pounding obtained using the ISEE method, which is considered as reference solution. The analytical estimates provide a very good estimate of the pounding risk for a wide range of separation distances. In this particular case, the results obtained using the mVM hazard function give the best approximation of the ISEE results.

Fig. 8b compares the 50-year probability of pounding for the buildings before retrofit and after retrofit following the six different retrofit solutions considered in this application example. The results presented in Fig. 8b are obtained using the mVM approximation of the hazard function.

It is observed that the use of viscous dampers can be very effective in reducing the risk of pounding between the two buildings. It is also found that the introduction of viscous braces according to scheme 2 is a very efficient retrofit solution, since it obtains a significant reduction of the pounding risk at a significantly lower retrofit cost when compared with retrofit scheme 1. Furthermore, retrofit scheme 3 also achieves a good compromise between retrofit costs and reduction of pounding risk.

5. Conclusions

This paper presents a fully probabilistic performance-based methodology for assessment of the seismic pounding risk between adjacent buildings. This methodology, which is consistent with the PEER performance-based earthquake engineering framework, is able to account for all pertinent sources of uncertainty that can affect the pounding risk, e.g., uncertainty in the seismic input (i.e., site hazard and record-to-record variability) and in the parameters used to describe the structural systems of interest (i.e., material properties, geometry, damping properties, and separation distance).

An efficient combination of analytical and simulation techniques is proposed for the calculation of the pounding risk under the assumptions of linear elastic behavior for the buildings and of non-stationary Gaussian input ground motion. The pounding problem is recast as a first-passage reliability problem, which is solved analytically by using the spectral characteristics (up to the

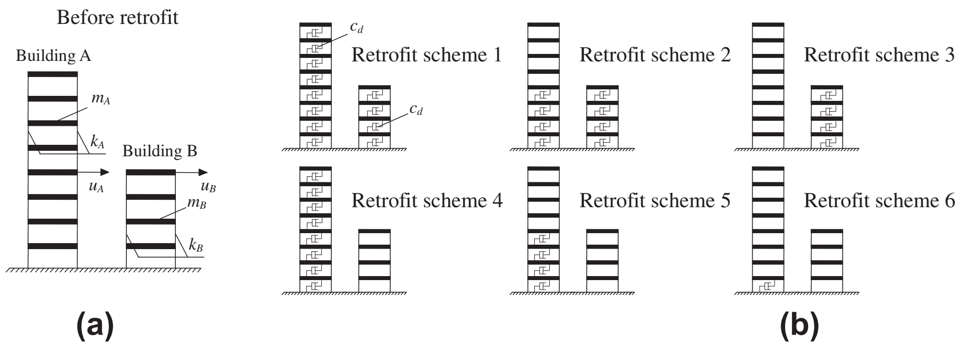

Fig. 7. Pounding risk between multistory buildings A and B: (a) buildings before retrofit, and (b) different retrofit schemes.

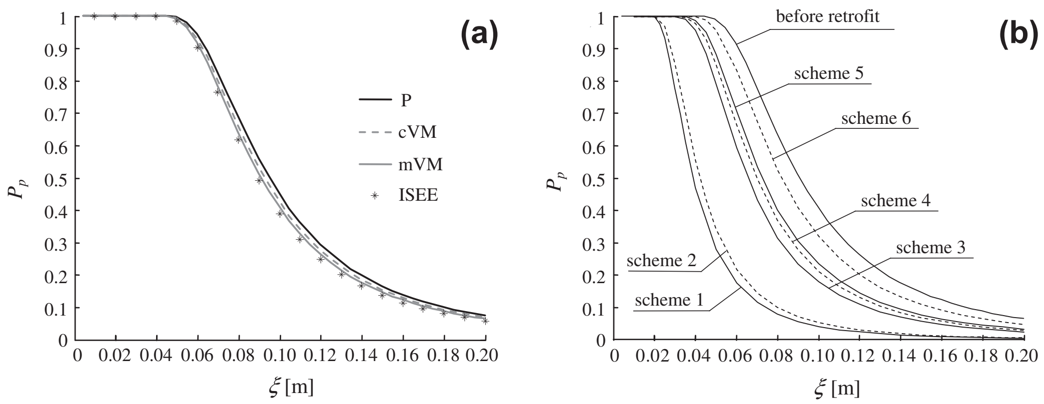

Fig. 8. Pounding risk between multistory buildings A and B: (a) comparison of different analytical solution and ISEE results, and (b) comparison of different retrofit schemes.

second order) of the non-stationary stochastic process representing the relative displacement between the buildings. Three different analytical approximations of the time-variant hazard function are considered: (1) the Poisson's approximation, (2) the classical Vanmarcke's approximation, and (3) the modified Vanmarcke's approximation. Results obtained by employing the importance sampling using elementary events method are assumed as reference solutions to evaluate the absolute and relative accuracy of the three analytical approximations considered here. The proposed formulation is very convenient in the case of linear elastic multi-degree-of-freedom systems with both proportional and non-proportional damping, since the spectral characteristics of the relative displacement processes can be computed in exact closed form. The effects of uncertainty in the model parameters are efficiently included by means of the total probability theorem and the Latin hypercube sampling technique.

The proposed methodology is applied to investigate the risk of pounding between single-degree-of-freedom systems, both with deterministic and uncertain properties. With reference to this specific application example, the following observations are made. (1) The proposed combination of analytical and simulation techniques provides sufficiently accurate estimates of the pounding risk when the Vanmarcke's approximations are used to estimate the time-variant hazard function. It is noteworthy that, in general, the relative accuracy of the classical and modified Vanmarcke's approximations can be evaluated only on a case-by-case basis. (2) The accuracy of the analytical approximations of the time-variant hazard function depends on the ratio between the natural periods of the adjacent buildings. Higher accuracy is reached when the natural periods of the two buildings are well separated. (3) The Poisson's approximation of the time-variant hazard function yields always conservative estimates of the risk. (4) Neglecting the effects of model parameter uncertainty can induce an underestimation of the pounding risk. Therefore, it is recommended that model parameter uncertainty, often neglected in previous studies, be considered in the pounding risk assessment.

In addition, the capabilities of the proposed method are demonstrated by assessing the effectiveness of the use of viscous dampers, according to different retrofit schemes, in reducing the pounding probability of adjacent multistory buildings modeled as linear elastic multi-degree-of-freedom systems. Based on the results presented, the following considerations are made for the application example considered in this paper. (1) The analytical approximations provide very accurate estimates of the pounding risk, due to the fact that the fundamental periods of the two buildings are well separated. (2) The use of viscous dampers can dramatically reduce the risk of pounding between the two systems for any given separation distance. (3) The use of viscous braces in the lower levels of the shorter building is a very efficient and cost-effective technique for minimizing the pounding risk.

Based on the results presented in this paper, it is concluded that the proposed methodology can be efficiently employed (1) for the assessment of pounding risk of adjacent buildings exhibiting linear elastic behavior before pounding, (2) for the computation of the mean annual frequency of pounding between adjacent buildings in the context of performance-based earthquake engineering, and (3) for the rational evaluation of the absolute and relative effectiveness of different retrofit solutions for adjacent building with high risk of seismic pounding.

Acknowledgements

The authors gratefully acknowledge support of this research by (1) the Louisiana Board of Regents (LA BoR) through the Pilot

Funding for New Research (Pfund) Program of the National Science Foundation (NSF) Experimental Program to Stimulate Competitive Research (EPSCoR) under Award No. LEQSF(2011)-PFUND-225; (2) the LA BoR through the Louisiana Board of Regents Research and Development Program, Research Competitiveness (RCS) subprogram, under Award No. LESQSF(2010-13)-RD-A-01; (3) the Longwell's Family Foundation through the Fund for Innovation in Engineering Research (FIER) Program; and (4) the LSU Council on Research through the 2009–2010 Faculty Research Grant Program. Any opinions, findings, conclusions or recommendations expressed in this publication are those of the authors and do not necessarily reflect the views of the sponsors.

References

[1] Jeng V, Kasai K, Maison BF. A spectral difference method to estimate building separations to avoid pounding. Earthquake Spectra 1992;8:201–23.
[2] Kasai K, Jagiasi AR, Jeng V. Inelastic vibration phase theory for seismic pounding mitigation. ASCE J Struct Eng 1996;122:1136–46.
[3] Penzien J. Evaluation of building separation distance required to prevent pounding during strong earthquakes. Earthquake Eng Struct Dynam 1997;26:849–58.
[4] ICBO. Uniform Building Code. Whittier, California: International Conference of Building Officials; 1997.
[5] Lopez-Garcia D, Soong TT. Assessment of the separation necessary to prevent seismic pounding between linear structural systems. Probab Eng Mech 2009;24:210–23.
[6] Lin JH. Separation distance to avoid seismic pounding of adjacent buildings. Earthquake Eng Struct Dynam 1997;26:395–403.
[7] Lin JH, Weng CC. Probability analysis of seismic pounding of adjacent buildings. Earthquake Eng Struct Dynam 2001;30:1539–57.
[8] Hong HP, Wang SS, Hong P. Critical building separation distance in reducing pounding risk under earthquake excitation. Struct Saf 2003;25:287–303.
[9] Wang SS, Hong HP. Quantiles of critical separation distance for nonstationary seismic excitations. Eng Struct 2006;28:985–91.
[10] Porter KA. An overview of PEER's performance-based earthquake engineering methodology. In: 9th International conference on application of statistics and probability in civil engineering (ICASP9). San Francisco, California; 2003. p. 973–80.
[11] Zhang Y, Acero G, Conte JP, Yang Z, Elgamal A. Seismic reliability assessment of a bridge ground system. In: 13th World conference on earthquake engineering. Canada: Vancouver; 2004.
[12] Luco N, Cornell CA. Structure-specific scalar intensity measures for near-source and ordinary earthquake ground motions. Earthquake Spectra 2007;23:357–92.
[13] Karayannis CG, Favvata MJ. Earthquake induced interaction between adjacent reinforced concrete structures with non equal heights. Earthquake Eng Struct Dynam 2005;34:1–20.
[14] Jankowski R. Non linear viscoelastic modelling of earthquake induced structural pounding. Earthquake Eng Struct Dynam 2005;34:595–611.
[15] Muthukumar S, DesRoches R. A Hertz contact model with non linear damping for pounding simulation. Earthquake Eng Struct Dynam 2006;35:811–28.
[16] Cole G, Dhakal R, Carr A, Bull D. An investigation of the effects of mass distribution on pounding structures. Earthquake Eng Struct Dynam 2011;40:641–59.
[17] Roberts JB, Spanos PD. Random vibration and statistical linearization. Dover Pubns; 2003.
[18] Au SK, Beck JL. Estimation of small failure probabilities in high dimensions by subset simulation. Probab Eng Mech 2001;16:263–77.
[19] Crandall SH. First-crossing probabilities of the linear oscillator. J Sound Vib 1970;12:285–99.
[20] Wen YK. Approximate methods for nonlinear time-variant reliability analysis. ASCE J Eng Mech 1987;113:1826–39.
[21] Vanmarcke E. On the distribution of the first-passage time for normal stationary random processes. J Appl Mech 1975;42:215–20.
[22] Barbato M. Use of time-variant spectral characteristics of nonstationary random processes in structural reliability and earthquake engineering applications. In: M Papadrakakis GS, Papadopoulos V. editors. Computational methods in stochastic dynamics. Springer; 2011.
[23] Michaelov G, Sarkani S, Lutes LD. Spectral characteristics of nonstationary random processes – A critical review. Struct Saf 1999;21:223–44.
[24] Barbato M, Conte JP. Spectral characteristics of non-stationary random processes: theory and applications to linear structural models. Probab Eng Mech 2008;23:416–26.
[25] Barbato M, Vasta M. Closed-form solutions for the time-variant spectral characteristics of non-stationary random processes. Probab Eng Mech 2010;25:9–17.
[26] Lai SP. Statistical characterization of strong ground motions using power spectral density function. Bull Seismol Soc Am 1982;72:259–74.
[27] Nuti C, Vanzi I. Influence of earthquake spatial variability on differential soil displacements and SDF system response. Earthquake Eng Struct Dynam 2005;34:1353–74.
[28] Marano GC, Greco R, Mezzina M. Stochastic approach for analytical fragility curves. KSCE J Civil Eng 2008;12:305–12.
[29] Der Kiureghian A, Fujimura K. Nonlinear stochastic dynamic analysis for performance-based earthquake engineering. Earthquake Eng Struct Dynam 2009;38:719–38.
[30] Vamvatsikos D, Cornell CA. Incremental dynamic analysis. Earthquake Eng Struct Dynam 2002;31:491–514.
[31] Hao H, Zhang SR. Spatial ground motion effect on relative displacement of adjacent building structures. Earthquake Eng Struct Dynam 1999;28:333–49.
[32] Lutes LD, Sarkani S. Stochastic analysis of structural and mechanical vibration. Upple Saddle River, NJ: Prentice Hall; 1997.
[33] Barbato M, Conte JP. Structural reliability applications of spectral characteristics of non-stationary random processes. ASCE J Eng Mech 2011. doi:10.1061/(ASCE)EM.1943-7889.0000238.
[34] Ghazizadeh S, Barbato M, Tubaldi E. A new analytical solution of the first-passage reliability problem for linear oscillators. ASCE J Eng Mech 2012. doi:10.1061/(ASCE)EM.1943-7889.0000365.
[35] Au SK, Beck JL. First excursion probabilities for linear systems by very efficient importance sampling. Probab Eng Mech 2001;16:193–207.
[36] Iman RL, Conover WJ. Small sample sensitivity analysis techniques for computer models, with an application to risk assessment. Commun Statist 1980:1749–842.
[37] Shinozuka M, Sato Y. Simulation of nonstationary random processes. ASCE J Eng Mech Div 1967;93:11–40.
[38] Clough RW, Penzien J. Dynamics of structures. New York: McGraw-Hill; 1993.
[39] Shome N, Cornell CA, Bazzurro P, Carballo JE. Earthquake, records, and nonlinear responses. Earthquake Spectra 1998;14:469–500.
[40] Tubaldi E, Barbato M, Dall'Asta A. Influence of model parameter uncertainty on seismic transverse response and vulnerability of steel-concrete composite bridges with dual load path. ASCE J Struct Eng 2012. doi:10.1061/(ASCE)ST.1943-541X.0000456.
[41] Bazzurro P. Probabilistic seismic demand analysis, Ph.D. Dissertation, department of civil and environmental engineering, stanford university. California; 1998. <http://pitch.stanford.edu/rmsweb/Thesis/PaoloBazzurro.pdf>.
[42] Baker JW, Cornell CA. Vector-valued intensity measures incorporating spectral shape for prediction of structural response. J Earthquake Eng 2008;12:534–54.
[43] Shinozuka M, Deodatis G. Simulation of stochastic processes by spectral representation. Appl Mech Rev 1991;44:191–203.
[44] Cornell CA, Jalayer F, Hamburger R, Foutch D. Probabilistic basis for 2000 SAC federal emergency management agency steel moment frame guidelines. ASCE J Struct Eng 2002;128:526–32.
[45] ECS. Eurocode 8: design of structures for earthquake resistance–Part 2: Bridges. EN1998. European Committee for Standardization; 2005.
[46] Lubkowski Z. Deriving the seismic action for alternative return periods according to Eurocode 8. In: 14th European conference on earthquake engineering. Ohrid, Macedonia; 2010.
[47] Toro GR, Cornell CA. Extremes of Gaussian processes with bimodal spectra. ASCE J Eng Mech 1986;112:465–84.
[48] JCSS. Probabilistic model code for reliability based design. Joint Committee on Structural Safety; 2001.
[49] Lin JH. Evaluation of seismic pounding risk of buildings in Taiwan. Chin Inst Eng 2005;28:867–72.
[50] Occhiuzzi A. Additional viscous dampers for civil structures: analysis of design methods based on effective evaluation of modal damping ratios. Eng Struct 2009;31:1093–101.